

RESEARCH

Open Access



Force distributions associated with different elastic traction methods for maxillary dentition distalization by clear aligners: an in-vitro study

Baolong Song^{1†}, Yizhe Qi^{2†}, Jianwei Sun², Zexu Gu^{2*} and Rui Liu^{1*}

Abstract

Objective The aim of this study was to examine the distribution patterns of orthodontic and reactive forces on each tooth during dentition distalization using clear aligners (CAs), and to assess the impact of different elastic traction methods.

Materials and methods Three sets of aligners for maxillary dentition distalization were fabricated, targeting different tooth movements: simultaneous distalization of the first molars and second premolars; simultaneous distalization of the first premolars and canines; and simultaneous retraction of incisors. An in vitro orthodontic simulator, consisting of 14 three-dimensional sensors, was used to evaluate mechanical changes in each tooth. The orthodontic and reactive forces exerted by aligners, along with additional pulling forces from 1/4 inch 3.5oz elastic using different elastic traction methods (with hooks or buttons), were measured and subjected to comparative analysis.

Results The initial orthodontic force exerted by CAs varied across different teeth, ranging from 1.52 N to 6.77 N. Concurrently, the primary anchorage teeth experience reactive forces within a range of 1 N to 6.48 N. While the traction force on these teeth generally remained significantly smaller, staying below 0.6 N. The traction force exerted via hooks decayed to 84.3% and was primarily concentrated on the canines, whereas traction force applied via buttons transmitted approximately 96.1% and was more readily distributed to other teeth.

Conclusion Elastic traction is not sufficient to completely counteract the initial reactive forces produced by the deformation of CAs. It is advisable to use stronger elastics or extend aligner wear time to ensure sufficient anchorage protection. Utilizing traction with buttons can reduce mechanical loss and enhance the transmission of traction force to other teeth.

Keywords Orthodontic appliances, Clear aligners, Force, Thermoplastic appliance, Latex elastics

[†]Baolong Song and Yizhe Qi contribute equally to the work.

*Correspondence:

Zexu Gu

zeki99@163.com

Rui Liu

liurui123@tmmu.edu.cn

¹Department of Stomatology, Daping Hospital, Army Medical University (The Third Military Medical University), Chongqing 400042, China

²State Key Laboratory of Oral & Maxillofacial Reconstruction and Regeneration, National Clinical Research Center for Oral Diseases, Shaanxi Clinical Research Center for Oral Diseases, Department of Orthodontics, School of Stomatology, The Fourth Military Medical University, Xi'an 710032, Shaanxi, China



© The Author(s) 2025. **Open Access** This article is licensed under a Creative Commons Attribution-NonCommercial-NoDerivatives 4.0 International License, which permits any non-commercial use, sharing, distribution and reproduction in any medium or format, as long as you give appropriate credit to the original author(s) and the source, provide a link to the Creative Commons licence, and indicate if you modified the licensed material. You do not have permission under this licence to share adapted material derived from this article or parts of it. The images or other third party material in this article are included in the article's Creative Commons licence, unless indicated otherwise in a credit line to the material. If material is not included in the article's Creative Commons licence and your intended use is not permitted by statutory regulation or exceeds the permitted use, you will need to obtain permission directly from the copyright holder. To view a copy of this licence, visit <http://creativecommons.org/licenses/by-nc-nd/4.0/>.

Introduction

In recent years, more people have sought clear aligner therapy (CAT) for aesthetic and comfort reasons. CAs are increasingly used for the treatment of Class II malocclusions, particularly for molar distalization, which is an effective non-extraction treatment option for class II malocclusions with mild crowding. Through sequential distalization protocols, the biomechanical design of CAs can achieve bodily movement of molars by 1.5 mm without remarkable crown tipping or vertical movements [1]. However, this process inherently generates reactive forces on the adjacent teeth, leading to labial displacement and proclination of anterior teeth [2]. This phenomenon underlines the dual nature of CAs' force delivery system—while their thermoplastic properties allow precise control over the molar movement [3], the absence of rigid anchorage increases the stress redistribution on the anterior regions, especially in cases requiring molars' distalization more than 3 mm [4].

In previous biomechanical studies of CAs, a single 3D force and moment sensor (Nano 17; ATI Industrial Automation, Apex, NC, USA) was used to investigate the forces and moments of CAs on incisor translation, incisor rotation, and molar distalization on the specific tooth [5–7]. The 3D mechanical measurement platform with multiple sensors allows for the study of the force and moment variations on multiple teeth under different materials or different force application designs [8–10]. Through an in vitro study, Kaur H [11] reported that the reactive forces acting on anchorage teeth adjacent to the displaced tooth were of clinical significance and exerted opposing directions. Existing evidence suggests that non-distalizing teeth are inherently subjected to mesially directed counterforces during activation of CAs. However, current experimental models exhibit significant limitations, including oversimplification of multi-tooth biomechanical interactions, inadequate representation of force gradients throughout the dental arch, and insufficient precision in quantifying reactive forces exerted on anchorage teeth.

The clinical predictability of molar distalization in CA therapy relies to some extent on latex elastic traction, which serves as the cornerstone biomechanical strategy for anchorage reinforcement during posterior segment retraction [12, 13]. However, the biomechanical interplay between CA-generated stresses and elastic traction compensation remains mechanistically undefined.

This investigation advances two fundamental biomechanical hypotheses: (1) The directly applied elastic traction forces demonstrate a significant counteractive effect against the aligner-induced reactive forces exerted on individual anchorage teeth; (2) Bonded composite buttons exhibit significantly enhanced stress transfer efficiency compared to laser-cut aligner hooks during

orthodontic force application (Fig. 1). Using a multi-sensor biomechanical platform, this study systematically quantifies real-time force distributions across the maxillary dentition, while comparatively analyzing baseline forces during CA activation with elastic traction-induced compensatory forces to elucidate anchorage preservation mechanisms. Furthermore, two clinical traction modalities—precision laser-cut CA hooks and bonded composite traction buttons—are biomechanically evaluated to characterize their stress redistribution efficacy. The findings aim to establish an evidence base for optimizing elastic traction protocols, thereby mitigating adverse anterior displacement while maintaining predictable molar distalization.

Materials and methods

This in-vitro study simulated CA therapy for Class II malocclusion correction through 2 mm full-arch maxillary distalization. Sequential distalization protocols were digitally planned using ATreat Designer V3.0 (Wuxi EA Medical Instruments Technologies, China) on a standardized maxillary model (NISSIN PE-ANA009), implementing the classical V-pattern strategy with 0.2 mm incremental tooth movements per clinical stage. Vertical rectangular attachments (3 × 2 × 1 mm) were bonded to bilateral canines, premolars, and second molars, while first molars remained attachment-free [14, 15]. Three biomechanically distinct treatment phases were chosen as groups:

Group A (Posterior segment distalization) Bilateral first molars and second premolars underwent synchronized 0.2 mm distal movement.

Group B (Middle segment distalization) Bilateral first premolars and canines initiated coordinated 0.2 mm distal displacement.

Group C (Anterior retraction) All incisors executed 0.2 mm lingual retraction.

Each treatment group was further divided into three subgroups to evaluate traction modalities: control subgroups (A0, B0, C0; $n = 10$ aligners/group) without traction devices, intervention subgroups with precision laser-cut resin hooks (A1, B1, C1; $n = 10$ aligners/group) positioned at the canine gingival margin, and intervention subgroups with bonded composite traction buttons (A2, B2, C2; $n = 10$ aligners/group) placed at the mesial contact area of the canines, as detailed in Table 1; Fig. 1.

The number of aligners per group was determined via precision-driven methodology to ensure measured forces reflect true biomechanical properties within a ± 0.05 N error. The pre-experimental data for canine forces in Group A1 showed a total variability of $s = 0.057$ N,

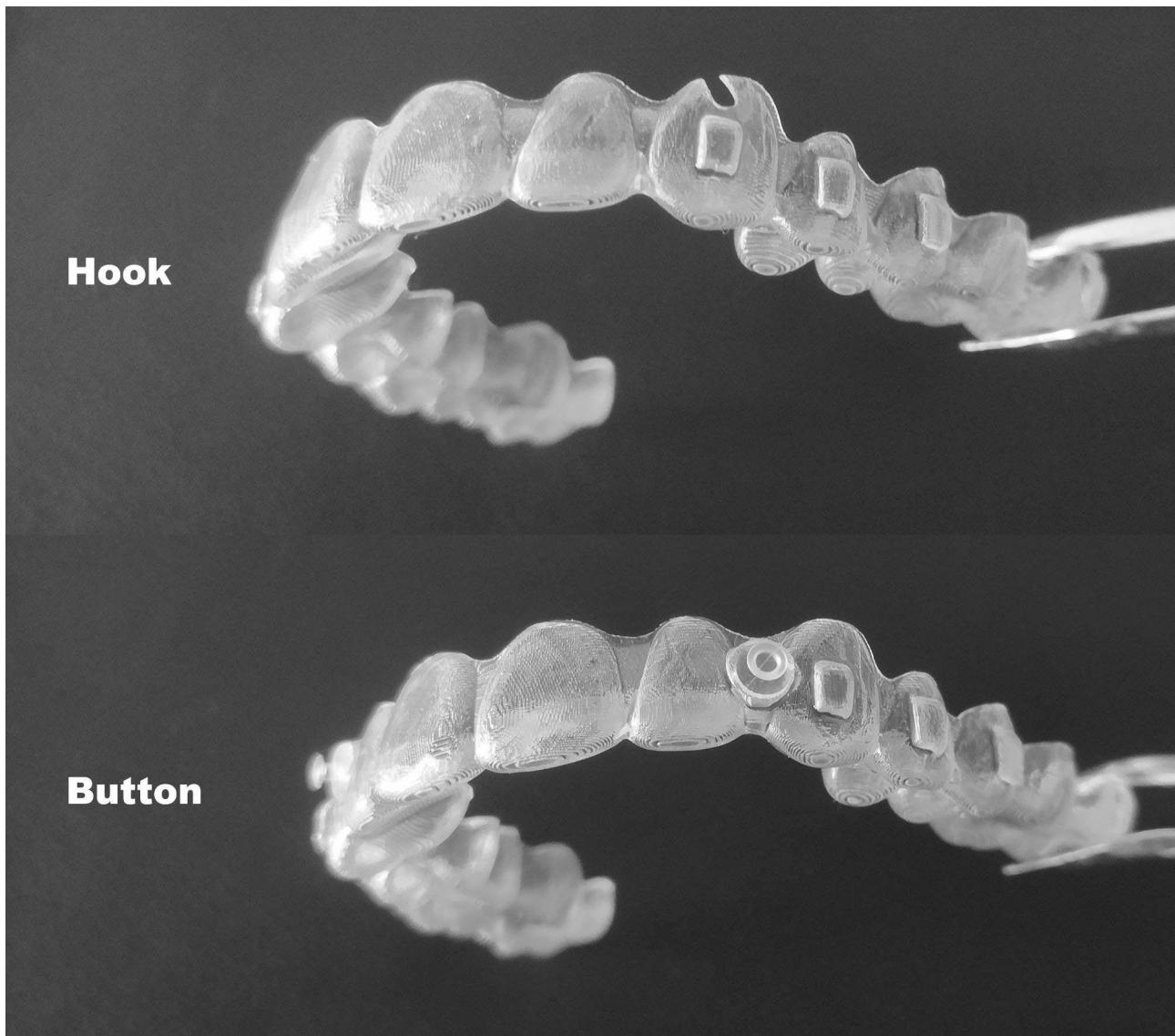


Fig. 1 Two different methods for elastic traction. (In the Hook group, the edges of the aligner were cut in the region of the maxillary canine; for the Button group, two pre-made buttons were adhered to the mesial area of the canines.)

Table 1 Grouping information on aligners and traction methods

Groups	Amount of activation(mm)	Mode of traction	Latex elastics size	Sample size
A0	15, 16, 25, 26 distalization 0.2	-	-	10
A1	15, 16, 25, 26 distalization 0.2	hook	1/4" 3.5Oz	10
A2	15, 16, 25, 26 distalization 0.2	button	1/4" 3.5Oz	10
B0	13, 14, 23, 24 distalization 0.2	-	-	10
B1	13, 14, 23, 24 distalization 0.2	hook	1/4" 3.5Oz	10
B2	13, 14, 23, 24 distalization 0.2	button	1/4" 3.5Oz	10
C0	11, 12, 21, 22 retraction 0.2	-	-	10
C1	11, 12, 21, 22 retraction 0.2	hook	1/4" 3.5Oz	10
C2	11, 12, 21, 22 retraction 0.2	button	1/4" 3.5Oz	10

resulting from combined machining and measurement errors. Based on a 95% confidence interval ($Z=1.96$), a theoretical requirement of 6 aligners per group was calculated. To address potential instability in the thermal forming process, 10 aligners per subgroup were ultimately processed, achieving an actual margin of error of 0.035 N. Within each subgroup, all 10 aligners were fabricated from identical CAD models (intra-subgroup design consistency) through independent 3D printing and thermoforming workflows, using 0.76 mm PET-G material (Duran®, Scheu Dental GmbH).

The corresponding maxillary arch configurations (different interdental spaces in Groups A/B/C) were instrumented with 14 Nano17 six-axis load cells (ATI Industrial Automation, Apex, NC, USA), rigidly affixed to each tooth via custom-milled titanium abutments (Fig. 2). To minimize errors in the assembly and fabrication of CAs, it is essential to perform force calibration and zeroing using a non-loading retainer prior to the commencement of formal measurements. The orthodontic force exerted on each tooth by the CAs was measured in groups A0, B0, and C0. In the hook groups A1, B1, C1, and button groups A2, B2, and C2, measured forces from aligners were nullified via software compensation (MATLAB, version 2019b, MathWorks Inc., Natick, MA, USA), retaining only elastic traction contributions. Class II traction was simulated using 1/4-inch, 3.5 oz latex elastics (Ormco Corporation, Sybron Dental Specialties, California, USA), with an initial diameter of 6.4 mm. The coordinate origin of the forces measured on each tooth were adjusted to the predicted resistance center, which was defined as the center of the root cross-section at the 1/3 point from the root tip, and the force direction was calibrated using the overall dental arch coordinates

as reference (Fig. 3). This study primarily focuses on the forces acting on the teeth along the Y-axis, which is parallel to the sagittal direction of the dental arch.

The data were presented as mean \pm SD and analyzed using SPSS 23.0 for statistical significance. Independent sample t-test was performed to compare two traction methods. One-way ANOVA analysis was performed followed by Bonferroni's test to analyze the comparison among different latex elastics. The significance level was set at $P<0.05$.

Results

Table 2 presents the force measurements exerted on all teeth using different aligners and tractions in the sagittal direction (F_y). A0, B0, and C0 represent the initial forces exerted on the teeth from aligner deformation, while A/B/C1-2 indicate the forces received by the teeth under different latex elastic tractions.

Figure 4 illustrates the sagittal forces resulting from aligner deformation. The teeth designed for distal movement received obvious orthodontic forces, while other teeth subjected to reactive forces. Average forces for bilateral first molar and second premolar distalization were 6.77 N and 3.77 N, respectively. For first premolar and canine distalization, average forces were 4.13 N and 4.24 N, respectively. For incisor and lateral incisor retraction, forces were 3.03 N and 1.52 N, respectively. Incisor retraction force was significantly lower than distalization force in posterior teeth ($p<0.05$), despite both having 0.2 mm activation.

In Group A (posterior segment distalization), the total reactive force within the biomechanical system measured 21.87 N, with the second molar exhibiting peak mesial reactive forces (6.38 ± 1.84 N), followed by the

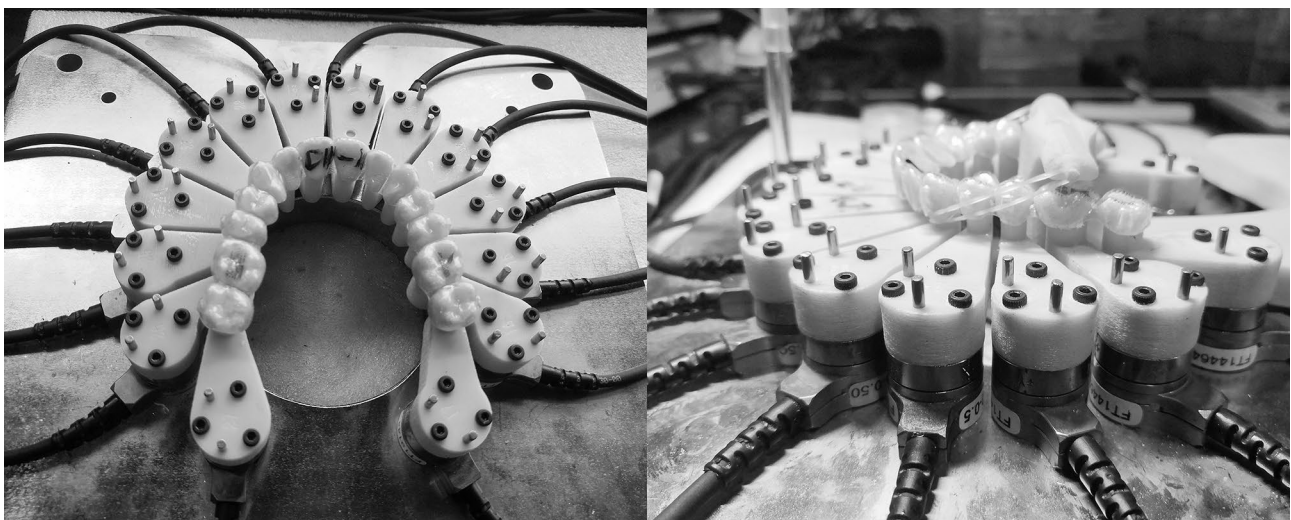


Fig. 2 Test apparatus and traction support. (Each tooth was securely connected to the Nano17 load sensor to monitor the real-time force applied to the tooth. The 3D-printed support was used to simulate Class II intraoral traction.)

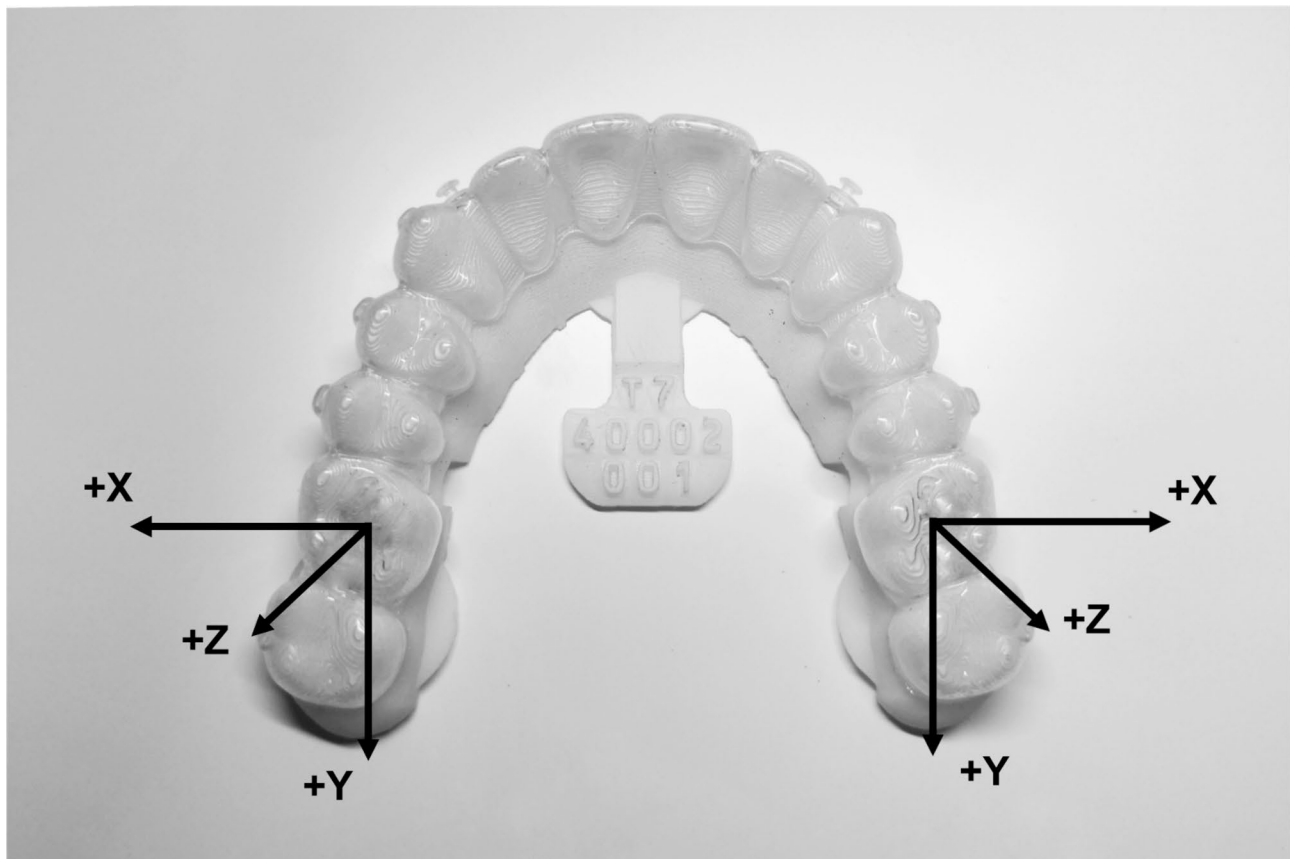


Fig. 3 Definitions of the coordinate axis. (The Y-axis was parallel with the sagittal direction of the dental arch, and force was presented in a positive value when directed backward.)

first premolar (1.72 ± 0.42 N) and canine (1.94 ± 0.58 N), while incisors experienced minimal protrusive forces (0.33 N, 0.57 N). Group B (middle segment distalization) demonstrated a 36.16% reduction in total reactive force (13.96 N), with non-movement planned teeth registering forces between 0.22 and 2.95 N ($P < 0.01$ vs. Group A, ANOVA). In Group C (anterior retraction), the total system reactive force decreased to 11.41 N, with posterior teeth generated passive anchorage forces of 0.58–1.93 N, reflecting a 18.27% reduction in anchorage demand compared to Group B at non-movement planned teeth.

The traction lengths for the hook and button groups were 28 mm and 31.3 mm, respectively, with the force value of the stretched elastics measured at 1.15 ± 0.06 N, showing no statistically significant differences. Figure 5 shows force variations with different tractions, with specific values provided in Table 2. In the hook group, the total actual traction force in the dentition was 1.95 N, representing 84.8% of the bilateral initial pulling force exerted by the elastics. Among these, the canine experienced the highest traction force at 0.37–0.62 N, followed by the second molar at 0.07–0.19 N, while the average traction force for the remaining teeth was less than 0.1 N. In the button group, the total traction force in the

dentition was 2.26 N, with 98.1% of the bilateral initial pulling force being transmitted. The canine experienced the highest traction force at 0.25–0.34 N, followed by the second molar at 0.17–0.23 N, while the other teeth also experienced traction forces ranging from 0.1 N to 0.2 N.

This study also examined the distribution of traction forces applied by different sizes of elastics (Supplementary Table S1). As the elastic force increases, the force exerted on each tooth correspondingly increases; however, it remains significantly smaller than the initial reactive forces caused by aligner deformation.

Discussion

During sequential distalization protocols using CAs, second molar movement can be effectively controlled through aligner biomechanical design alone [16]. However, anchorage reinforcement becomes critical when extending distal displacement to first molars or second premolars, as these orthodontic movements generate clinically significant reactive forces that may compromise treatment outcomes through undesirable anterior segment protrusion [1, 17]. Clinically, Class II elastic traction remains the primary method to counterbalance these reactive vectors through posteriorly directed forces [17].

Table 2 The force value in sagittal direction from different groups.

Groups	Fy on each tooth (N)																
	17	16	15	14	13	12	11	21	22	23	24	25	26	27			
A0 aligner force	-6.28±2.13	6.30±0.71	4.35±0.98	-1.48±0.40	-1.94±0.58	-0.39±0.30	-0.66±0.55	-0.48±0.49	-0.27±0.24	-1.94±0.59	-1.96±0.29	3.19±0.54	7.24±0.79	-6.48±1.48			
A1 hook traction force	0.13±0.03*	0.11±0.02	0.09±0.01	0.09±0.02*	0.37±0.06	0.08±0.01*	0.09±0.01*	0.01±0.03*	0.01±0.03*	0.45±0.05*	0.12±0.02*	0.06±0.03*	0.09±0.03	0.16±0.03*			
A2 button traction force	0.19±0.04	0.11±0.02	0.11±0.02	0.15±0.01	0.33±0.03	0.00±0.02	0.14±0.02	0.07±0.04	0.08±0.02	0.34±0.03	0.18±0.01	0.12±0.02	0.11±0.03	0.23±0.02			
B0 aligner force	-2.60±0.67	-0.22±0.5	-0.89±0.19	4.48±0.42	3.27±0.59	-0.98±0.27	-2.95±0.56	-1.59±0.93	-1.19±0.38	5.22±0.42	3.77±0.53	-1.18±0.44	-1.47±0.78	-0.89±0.28			
B1 hook traction force	0.17±0.04*	0.11±0.03*	0.07±0.02*	0.10±0.02*	0.45±0.07*	0.07±0.01	0.09±0.03*	0.04±0.03*	0.02±0.03	0.62±0.11*	0.06±0.06*	0.04±0.02*	0.06±0.04*	0.07±0.03*			
B2 button traction force	0.21±0.03	0.19±0.04	0.13±0.01	0.16±0.03	0.25±0.04	0.08±0.07	0.21±0.08	0.08±0.04	0.01±0.05	0.30±0.04	0.13±0.03	0.14±0.04	0.13±0.02	0.23±0.06			
C0 aligner force	-1.93±0.58	-0.78±0.68	-1.01±0.44	-0.58±0.55	-1.16±0.67	1.94±0.45	3.50±0.33	2.56±0.67	1.10±0.41	-1.63±1.12	-0.63±0.38	-1.15±0.45	-1.50±1.07	-1.04±0.43			
C1 hook traction force	0.19±0.03	0.12±0.01*	0.08±0.01*	0.08±0.03*	0.47±0.04*	0.08±0.02*	0.09±0.01*	0.05±0.01*	0.03±0.02	0.49±0.05*	0.08±0.02*	0.08±0.02*	0.07±0.02*	0.11±0.05*			
C2 button traction force	0.20±0.05	0.20±0.04	0.14±0.02	0.21±0.03	0.27±0.03	0.01±0.03	0.13±0.02	0.11±0.03	0.03±0.04	0.31±0.03	0.18±0.02	0.14±0.03	0.16±0.03	0.17±0.05			

* Significantly different from A/B/C 2 on the same tooth with t-test, P < 0.05

To systematically quantify these biomechanical interactions, we established three distinct treatment phases: Group A (posterior segment), Group B (middle segment), and Group C (anterior segment), each representing progressive distalization stages. Multi-axial force-moment sensors precisely mapped the real-time orthodontic forces and reactive force distribution across all maxillary teeth during these phases. Furthermore, comparative biomechanical analysis of elastic traction methods (hook vs. button) demonstrated distinct force distribution patterns, establishing an evidence-based protocol to match traction modalities with clinical anchorage requirements.

Initial orthodontic force and reactive force

The biomechanical foundation of CA dentition distalization therapy lies in sagittal displacement-induced interproximal space modulation: when programmed tooth movement alters proximal contact relationships, the resultant geometric discrepancy between the aligner and dentition upon seating creates localized elastic deformation [18]. This deformation generates reciprocal forces — acting on both the target tooth (via intentional strain energy storage) and adjacent teeth (through passive strain redistribution) — with vector orientations opposing the direction of aligner recovery [19]. The biomechanical heterogeneity observed in orthodontic force magnitudes arises from different aligner deformation mechanisms.

In groups A and B, first molar demonstrated significantly higher distalization forces (6.77 N) compared to premolars (3.77 N, 4.13 N) and canines (4.24 N), potentially attributable to its larger crown volume, which may increase the cross-sectional area of aligner deformation at mesial and distal contact surfaces, thereby amplifying strain energy generation. This morphological difference also contributed to Group A's elevated total reactive force (21.87 N vs. Group B: 13.95 N), suggesting heightened anchorage control requirements.

Group C exhibited further reductions in incisor retraction forces (1.52–3.03 N) and total system reactivity (11.41 N) relative to Group B. Mechanistically, anterior retraction engaged two deformation zones at the distal aspects of lateral incisors, whereas Group B's middle-segment distalization involved four deformation zones: mesial aspects of canines and distal aspects of first premolars bilaterally. This halved deformation zone quantity directly reduced elastic energy storage capacity.

Force vector analysis quantified differential anchorage demands, with Group A requiring 2.3-fold greater total posterior anchorage than Group C. These findings emphasize two biomechanical principles: Deformation quantity (number of activation zones) and deformation area size (crown dimensions modulating elastic energy storage) collectively govern force generation. Clinically, anchorage reinforcement protocols should be tailored

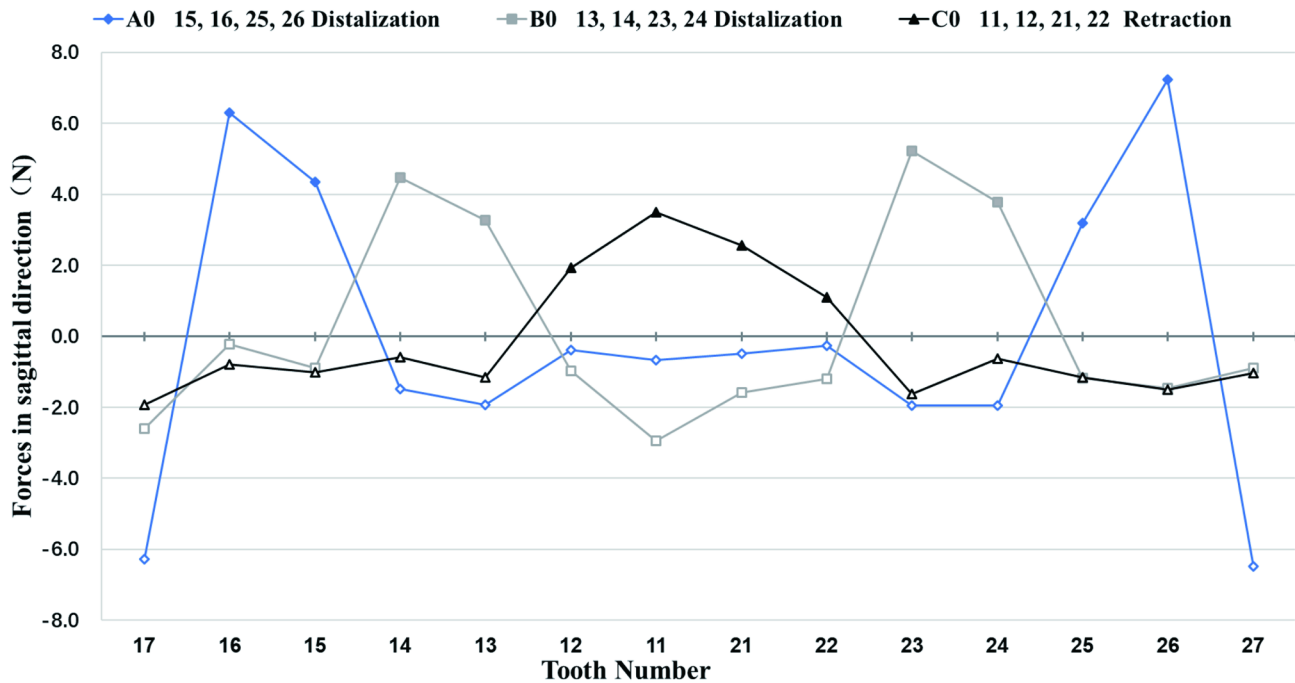


Fig. 4 Sagittal forces experienced by maxillary teeth during distalization across three groups. (The teeth designed for distal movement are marked in red.)

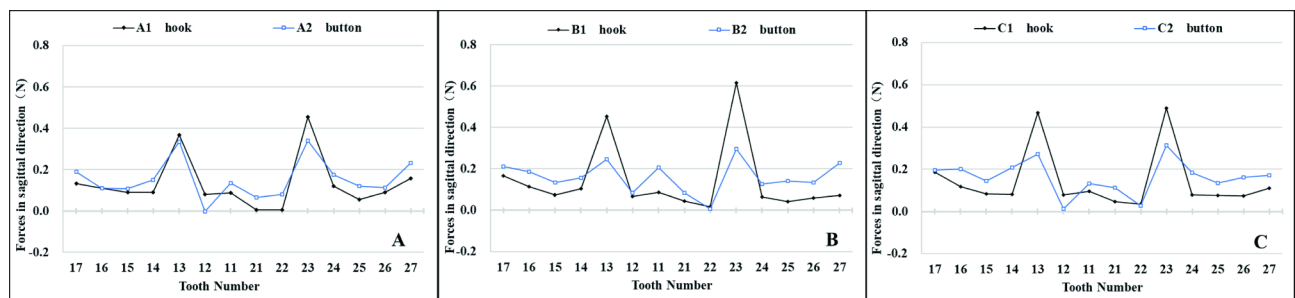


Fig. 5 Comparison of sagittal forces applied to maxillary teeth using two traction methods. (A: Simultaneous distalization of the first molars and second premolars; B: Simultaneous distalization of the first premolars and canines; C: Simultaneous retraction of incisors.)

to deformation patterns (quantity and morphology) observed during specific treatment phases, enabling precise biomechanical control aligned with aligner activation characteristics.

Simon et al. [14] quantified molar distalization forces via sensor measurements, reporting average values of 1.1 ± 0.8 N (with attachments) and 0.8 ± 0.7 N (without attachments). The lower measured force values may be attributed to the sensor’s movable design, which induces micromovement of teeth during force application, thereby dampening the instantaneous force peaks. Elk-holy’s in-vitro study demonstrated that a 0.75 mm-thick aligner generated 4.49 N of force for 0.25 mm incisor palatal displacement [20], aligning with our experimental force ranges. Crucially, these in-vitro measurements reflect initial force peaks arising from aligner deformation, whereas actual intraoral forces transmitted to teeth are attenuated — periodontal ligament (PDL)

hydrodynamics mediate force redistribution through physiological tooth displacement [21].

During Group A’s molar/premolar distalization, the second molars — as the sole anchorage units in the distal arch — sustained equivalent mesial reactive forces (6.38 ± 1.84 N) to the applied distalization forces, creating reciprocal mesialization risks. Conversely, reactive forces in the mesial arch dissipated through a force dissipation gradient, progressing from the first premolars and canines (1.72–1.94 N) to the incisors (0.33–0.57 N) (Fig. 4). In Group B’s premolar/canine distalization, the incisor region experienced significant reactive forces (1.09–2.27 N), necessitating reinforced anterior anchorage devices. In Group C, the incisor retraction generated forward reactive forces that were relatively uniformly distributed across posterior anchorage teeth in the distal arch (0.61–1.48 N), demonstrating coordinated force-sharing through collective anchorage contribution.

Experimental biomechanical data confirm the critical role of grouped anchorage mechanics in CA systems. Non-target teeth positioned mesially or distally relative to the aligner's deformation direction passively stabilize as anchorage groups. As these groups expand in tooth number, the reactive force distributed to each anchorage unit decreases proportionally.

The biomechanical principles highlighted in this study are further supported by parallel investigations in the field. Finite element analyses reveal that anchorage loss, including the labial movement of maxillary anterior teeth and the mesial movement of distalized maxillary posterior teeth, occurs during the maxillary dentition distalization process [4, 19, 22–24]. However, the application of elastic traction can mitigate anchorage loss and enhance the success of maxillary dentition distalization with CA. Specifically, the palatal mini-screw anchorage system demonstrates superior biomechanical characteristics and greater efficacy compared to the buccal mini-screw anchorage system [22, 24], with its effectiveness surpassing that of Class II elastics [24]. Theoretical models suggest that reducing the aligner coverage on the distal surfaces of molars during premolar distalization could effectively decrease anchorage loss and improve the overall efficiency of molar distalization [23], however, clinical application requires additional reinforcement of anterior anchorage. Additionally, according to the case report by Mario Greco et al. [16], micro-implants can be inserted and rigidly linked to the second molar following its distalization to the target position. This dual-action approach not only stabilizes the molar but also provides indirect anchorage for the anterior segment, thereby minimizing anchorage loss.

Reactive force and traction force

Contrary to our initial hypothesis, experimental data conclusively demonstrate that elastic traction forces applied to CAs fail to significantly counteract CA-induced reactive forces on anchorage teeth ($P < 0.01$). Quantitative analysis revealed that the maximum traction force (0.62 N) measured during elastic activation on canines amounted to only 32–53% of the initial reactive forces (1.16–1.94 N) generated by aligner deformation (Table 2). This critical insufficiency in force compensation directly explains the observed anchorage loss even when mini-screw implants were applied [4, 25, 26]. These findings refute Hypothesis 1, confirming that CA-generated reactive forces dominate the initial biomechanical system, while elastic traction serves primarily as a modulating rather than neutralizing influence.

However, in the actual clinical process, the balance between these two forces is continually shifting. The orthodontic force decreases over time until it disappears, due to tooth movement and mechanical degradation of

orthodontic materials [14, 27]. The reduction in elastic force is most pronounced during the first 1–2 h, after which the degradation of force value decreases steadily, consistently maintaining over 60% of the initial force value within 48 h [28, 29]. Therefore, by regularly replacing the latex elastics during the use of the same aligner, the traction force will progressively approach and ultimately exceed the reactive force.

To achieve a protective anchoring effect through traction, orthodontists can balance the force differences not only by reducing the activation amount per step or by replacing the elastic bands with those of greater strength, but also by adjusting the wearing time of each aligner to achieve temporal force balance. Moreover, we can leverage the inherent torque control advantages of CAs by applying strategic lingual crown torque to prevent labial tipping of anterior teeth [30].

Comparison of different traction methods

Our findings substantiate Hypothesis 2, demonstrating that bonded composite buttons achieve significantly higher force transmission efficiency (98.1% force retention) compared to laser-cut aligner hooks (84.8% force retention). This discrepancy stems from fundamental biomechanical principles: According to the Kirchhoff-Love thin plate theory [31], tension applied at the material's edge leads to higher bending stress, making the material more susceptible to elastic deformation. Strain energy accumulation predominantly localizes at the material's periphery in the hook group, inducing 15.2% force transmission loss through mechanical hysteresis. Conversely, central force application (button group) achieves 98.1% force transmission efficiency through optimized strain energy convergence, limiting parasitic energy loss to 1.9%. Therefore, the force applied to incisors, premolars, and molars in the button group is significantly higher ($p < 0.05$, Fig. 5).

The differences in traction force experienced by the canines are related to the localized deformation of the aligners by the hook traction. Additionally, in hook traction, a portion of the elastic band is secured between the aligner and the tooth, creating direct contact with the canine. This results in frictional force acting directly on the canines, increasing the tensile force applied to them.

Previous investigations into differential traction methodologies have predominantly relied on three-dimensional finite element analyses. Liu et al. [32] compared conventional buttons (bonded to canines) versus laser-cut aligner hooks, demonstrating that aligner-based traction application provides enhanced anterior and molar anchorage preservation. Ji L's comparative analysis of laser-cut hooks versus angle buttons (bonded to aligners) revealed that angle button traction achieves superior

sagittal control of anterior teeth while simultaneously optimizing horizontal and vertical molar control [25].

In summary, the traction force in the hook group is primarily concentrated on the canines. In contrast, button traction reduces force loss and enhances force transmission within the aligner, making it beneficial for preserving the anchorage of incisors and posterior teeth, ultimately facilitating optimal clinical outcomes. Furthermore, the use of elastic traction via buttons in clinical practice offers several additional advantages. Firstly, buttons can be placed on the canines and mandibular molars to avoid cutouts in the aligner, ensuring that the design of the attachments remains unaffected. Secondly, the application of traction via buttons is easier for patients to manage. Lastly, the adhesion of the button occurs during the aligner manufacturing process, which can save chair time.

Limitations

This study had several limitations. Firstly, the study utilized petroleum jelly to lubricate the surface of the models; however, it did not fully simulate the humidity of the oral environment. Secondly, the study concentrated on the initial force associated with the deformation of the aligner, necessitating further research to understand the variations in orthodontic and anchoring forces as tooth movement occurs. Finally, the study only simulated the force value and direction of Class II traction during static occlusion; thus, the effects of mouth opening and mandibular movement on traction force require further investigation.

Conclusions

This study systematically elucidates the biomechanical mechanisms underlying sequential distalization and elastic traction in CA therapy. Three treatment phases demonstrated distinct force distribution patterns, revealing that deformation quantity and deformation area size collectively determine orthodontic force and reactive force intensity. Non-target teeth positioned mesially or distally relative to the CA's deformation direction passively stabilize as anchorage groups, with reactive forces per tooth decreasing as anchorage groups expand in tooth number.

Hook-based traction concentrates forces primarily on canines, whereas button traction achieves superior force transmission efficiency by centralizing strain energy convergence, thereby distributing traction forces more effectively across multiple teeth.

Critically, elastic traction cannot fully counteract the initial reactive forces generated by CA deformation. To achieve better biomechanical equilibrium, clinicians must account for inherent force attenuation and phase-specific aligner wear duration during treatment planning.

Supplementary Information

The online version contains supplementary material available at <https://doi.org/10.1186/s12903-025-05985-5>.

Supplementary Material 1

Acknowledgements

We are grateful to Xiao Deng and Yikan Zheng for their assistance in orthodontic appliance fabrication and computer software support.

Author contributions

B.S. contributed to methodology, validation of results and investigation conduction, wrote the first draft of the paper; Y.Q. conducted formal analysis, review and editing of the paper; J.S. contributed to interpretation of data; Z.G. provided the data resources and supervision; R.L. contributed to curation and project administration. All authors read and approved the final manuscript.

Funding

This work was supported by the National Clinical Medical Research Center for Oral Diseases (LCB202409) and The Fourth Military Medical University Clinical Research Program (2022LC2238).

Data availability

The data that support the findings of this study will be available in [Figshare] at <https://doi.org/10.6084/m9.figshare.28737350.v1>.

Declarations

Ethics approval and consent to participate

Not applicable.

Consent for publication

Not applicable.

Competing interests

The authors declare no competing interests.

Received: 4 January 2025 / Accepted: 10 April 2025

Published online: 18 April 2025

References

- Inchingolo AM, Inchingolo AD, Carpentiere V, et al. Predictability of dental distalization with clear aligners: A systematic review[J]. *Bioengineering*. 2023;10(12):1390. <https://doi.org/10.3390/bioengineering10121390>
- Shen C, Park TH, Chung CH, et al. Molar distalization by clear aligners with sequential distalization protocol: A systematic review and meta-analysis[J]. *J Funct Biomaterials*. 2024;15(6):137. <https://doi.org/10.3390/jfb15060137>
- Rossini G, Parrini S, Castroflorio T, et al. Efficacy of clear aligners in controlling orthodontic tooth movement: A systematic review[J]. *Angle Orthod*. 2015;85(5):881–9. <https://doi.org/10.2319/061614-436.1>
- Liu X, Wu J, Cheng Y, et al. Effective contribution ratio of the molar during sequential distalization using clear aligners and micro-implant Anchorage: A finite element study[J]. *Prog Orthodont*. 2023;24(1):35. <https://doi.org/10.1186/s40510-023-00485-0>
- Hahn W, Engelke B, Jung K, Dathe H, Fialka-Fricke J, Kubein-Meesenburg D, et al. Initial forces and moments delivered by removable thermoplastic appliances during rotation of an upper central incisor. *Angle Orthod*. 2010. <https://doi.org/10.2319/033009-181.1>
- Elkholy F, Schmidt F, Jäger R, Lapatki BG. Forces and moments applied during derotation of a maxillary central incisor with thinner aligners: an in-vitro study. *Am J Orthod Dentofac Orthop*. 2017. <https://doi.org/10.1016/j.ajodo.2016.08.020>
- Wiechens B, Brockmeyer P, Erfurth-Jach T, Hahn W. Force delivery modification of removable thermoplastic appliances using Hilliard precision thermopliers for tipping an upper central incisor. *Clin Oral Investig*. 2022. <https://doi.org/10.1007/s00784-022-04560-4>

8. Liu Y, Hu W. Force changes associated with different intrusion strategies for deep-bite correction by clear aligners. *Angle Orthod*. 2018. <https://doi.org/10.2319/121717-864.1>
9. Spanier C, Schwahn C, Krey KF, Ratzmann A. Fused filament fabrication (FFF): influence of layer height on forces and moments delivered by aligners-an in vitro study. *Clin Oral Investig*. 2023. <https://doi.org/10.1007/s00784-023-04912-8>
10. Grant J, Foley P, Bankhead B, Miranda G, Adel SM, Kim KB. Forces and moments generated by 3D direct printed clear aligners of varying labial and lingual thicknesses during lingual movement of maxillary central incisor: an in vitro study. *Prog Orthod*. 2023. <https://doi.org/10.1186/s40510-023-00475-2>
11. Kaur H, Truong J, Heo G, Mah JK, Major PW, Romanyk DL. An in vitro evaluation of orthodontic aligner biomechanics around the maxillary arch. *Am J Orthod Dentofac Orthop*. 2021. <https://doi.org/10.1016/j.ajodo.2021.04.005>
12. Mohamed RN, Basha S, Al-Thomali Y. Maxillary molar distalization with miniscrew-supported appliances in class II malocclusion: A systematic review. *Angle Orthod*. 2018. <https://doi.org/10.2319/091717-624.1>
13. Lombardo L, Colonna A, Carlucci A, Oliverio T, Siciliani G. Class II subdivision correction with clear aligners using intermaxillary elastics. *Prog Orthod*. 2018. <https://doi.org/10.1186/s40510-018-0221-5>
14. Simon M, Keilig L, Schwarze J, Jung BA, Bourauel C. Forces and moments generated by removable thermoplastic aligners: incisor torque, premolar derotation, and molar distalization. *Am J Orthod Dentofac Orthop*. 2014. <https://doi.org/10.1016/j.ajodo.2014.03.015>
15. White DW, Julien KC, Jacob H, Campbell PM, Buschang PH. Discomfort associated with invisalign and traditional brackets: A randomized, prospective trial. *Angle Orthod*. 2017. <https://doi.org/10.2319/091416-687.1>
16. Greco M, Rossini G, Rombolà A. G-block: posterior anchorage device tads-supported after molar distalization with aligners: an adult case report[J]. *Int Orthod*. 2022;20(4):100687. <https://doi.org/10.1016/j.jortho.2022.100687>
17. Xulin Liu Y, Cheng W, Qin S, Fang W, Wang Y, Ma Z. Effects of upper-molar distalization using clear aligners in combination with class II elastics: a three-dimensional finite element analysis. *BMC Oral Health*. 2022. <https://doi.org/10.1186/s12903-022-02526-2>
18. Moutawakil AE. Biomechanics of aligners: literature review[J]. *Adv Dentistry Oral Health*. 2021;13(5). <https://doi.org/10.19080/ADOH.2020.13.555872>
19. Mao B, Tian Y, Xiao Y, et al. The effect of maxillary molar distalization with clear aligner: A 4D finite-element study with staging simulation[J]. *Prog Orthodont*. 2023;24(1):16. <https://doi.org/10.1186/s40510-023-00468-1>
20. Elkholy F, Panchaphongsaphak T, Kilic F, Schmidt F, Lapatki BG. Forces and moments delivered by PET-G aligners to an upper central incisor for labial and palatal translation. *J Orofac Orthop*. 2015. <https://doi.org/10.1007/s00056-015-0307-3>
21. Van Driel WD, van Leeuwen EJ, Von den Hoff JW, Maltha JC, Kuijpers-Jagtman AM. Time-dependent mechanical behaviour of the periodontal ligament. *Proc Inst Mech Eng H*. 2000. <https://doi.org/10.1243/0954411001535525>
22. Guo R, Li L, Lam XY, et al. Tooth movement analysis of maxillary dentition distalization using clear aligners with buccal and palatal mini-screw anchorages: A finite element study[J]. *Orthod Craniofac Res*. 2024;27(6):868–76. <https://doi.org/10.1111/ocr.12826>
23. Mao B, Tian Y, Liu D, Zhou Y, Wang S. The effect of maxillary premolar distalization with different designed clear aligners: a 4D finite element study with staging simulation. *Prog Orthod*. 2024;25(1):46. <https://doi.org/10.1186/s40510-024-00545-z>
24. Gao H, Luo L, Liu J. Three-dimensional finite element analysis of maxillary molar distalization treated with clear aligners combined with different traction methods. *Prog Orthod*. 2024;25(1):47. <https://doi.org/10.1186/s40510-024-00546-y>
25. Ji L, Li B, Wu X. Evaluation of biomechanics using different traction devices in distalization of maxillary molar with clear aligners: A finite element study[J]. *Comput Methods Biomech Biomed Eng*. 2023;26(5):559–67. <https://doi.org/10.1080/10255842.2022.2073789>
26. Qiang R, Zhang H, Xu Y, et al. Accuracy of maxillary molar distalization with clear aligners in three-dimension: A retrospective study based on CBCT superimposition[J]. *Clin Oral Invest*. 2025;29(2):138. <https://doi.org/10.1007/s00784-025-06218-3>
27. Ihssen BA, Willmann JH, Nimer A, Drescher D. Effect of in vitro aging by water immersion and thermocycling on the mechanical properties of PETG aligner material. *J Orofac Orthop*. 2019. <https://doi.org/10.1007/s00056-019-00192-8>
28. Kanchana P, Godfrey K. Calibration of force extension and force degradation characteristics of orthodontic latex elastics. *Am J Orthod Dentofac Orthop*. 2000. <https://doi.org/10.1067/mod.2000.104493>
29. Yang L, Lv C, Yan F, Feng J. Force degradation of orthodontic latex elastics analyzed in vivo and in vitro. *Am J Orthod Dentofac Orthop*. 2020. <https://doi.org/10.1016/j.ajodo.2019.03.028>
30. Nguyen VA, Nguyen TA. Recovery of incisor torque loss with clear aligners after lingual orthodontic treatment: A case report[J]. *J Aligner Orthod*. 2024;8:47–53.
31. Zhao X, Sun Z, Zhu Y, Yang C. Revisiting Kirchhoff–Love plate theories for thin laminated configurations and the role of transverse loads. *J Compos Mater*. 2022. <https://doi.org/10.1177/00219983211073853>
32. Liu X, Cheng Y, Qin W, et al. Effects of upper-molar distalization using clear aligners in combination with class II elastics: A three-dimensional finite element analysis[J]. *BMC Oral Health*. 2022;22(1):546. <https://doi.org/10.1186/s12903-022-02526-2>

Publisher's note

Springer Nature remains neutral with regard to jurisdictional claims in published maps and institutional affiliations.